A Wearable Neuro-Degenerative Diseases Classification System Using Human Gait Dynamics

Wala Saadeh$^{(\boxtimes)}$ and Muhammad Awais Bin Altaf

Electrical Engineering Department, Lahore University of Management Sciences,
Lahore, Pakistan
{wala.saadeh, awais.altaf}@lums.edu.pk

Abstract. The increasing prevalence of neurodegenerative diseases (NDDs) impose substantial medical and public health burdens on populations throughout the world. NDDs are chronic diseases that affect the human central nervous system causing loss of neurons within the brain and/or spinal cord. This causes deterioration in movement and mental functioning of the patients. The current medications for this group of disorders are limited and aim to treat the symptoms only. A better understanding of the mechanisms underlying neurodegeneration should lead to more effective, disease-modifying treatments in the future. Continuous assessment of NDD patients is a key element of future care and treatment. This contribution proposes a wearable NDD detection system based on patient's gait dynamics using an unobtrusive force resistive sensor embedded in patient's shoe. The NDD classification is based on 3 fundamental gait features: stride time, stride time's fluctuation and the autocorrelation decay factor. It is designed to discriminate between healthy subjects and NDD patients and moreover identify the NDD type: (Huntington's disease (HD), Parkinson Disease (PD), and Amyotrophic Lateral Sclerosis (ALS)). The proposed NDD classification algorithm is implemented on FPGA and verified experimentally using Gait Dynamics dataset from Physionet. It offers a classification accuracy of 93.8%, 89.1%, 94% and 93.3%, for ALS, HD, PD, and healthy person, respectively, from a total set of 64 subjects.

Keywords: Amyotrophic Lateral Sclerosis (ALS) · Huntington's disease · Parkinson Disease · Neurodegenerative disorders · Classifier · Wearable sensor

1 Introduction

Patients with Neurodegenerative diseases (NDDs) suffer from medical conditions that directly affect the neurons within the brain [1]. NDDs cause changes in neuromuscular control causing degradation in muscle movements control, muscle tone, involuntary movements and smoothness of movement. One of the key diagnostic approaches for defining the NDD is the study of patient's gait [2–4]. Parkinson's disease (PD), Huntington's disease (HD) and Amyotrophic Lateral Sclerosis (ALS) are the main types of NDDs deteriorating the patient's gait [1].

1.1   Parkinson's Disease

PD is a chronic and progressive movement disorder causing trembling in the hands, arms, legs, jaw, and face, stiffness the limbs and trunk, slowed movement, and impaired balance and coordination [5]. After Alzheimer, PD is the second most common neurodegenerative disease affecting approximately 1 million Americans (estimates range between 4 and 6.5 million people worldwide) and about 1% of older adults. It usually affects people over the age of 50 [5]. In the US alone, 60,000 new cases are diagnosed with PD each year. There is currently no accurate test for the diagnosis of PD and it is highly uncertain in the early stages of the disease. These symptoms usually begin gradually and worsen with time. The gait of PD patients is characterized by small shuffling steps and a general slowness of movement [3]. The stride length and walking speed during free ambulation are also reduced.

1.2   Huntington's Disease

HD is a genetic NDD that affects muscle coordination and leads to cognitive decline and physical, mental and emotional changes [6]. It is estimated that around 30,000 people in the US only are affected by HD, and more than 150,000 people have $\sim 50\%$ potential risk of developing HD. Patients with HD are not able to think, talk and move properly [6, 7]. This disease is responsible for destroying the cells in the basal ganglia, the part of the brain that controls these capacities. HD usually develops at mid-age and can cause a very wide range of symptoms. The general symptoms in early stages can include a poor memory; difficulty in making decisions; mood changes such as depression, anger or irritability; a growing lack of coordination, twitching or other uncontrolled movements; difficulty in walking, speaking or swallowing [8, 9].

1.3   Amyotrophic Lateral Sclerosis (ALS)

ALS is known as motor neuron disease characterized by progressive weakness, difficulty in speaking, swallowing, breathing, muscle twitching (involuntary muscle contraction and relaxation), and muscle stiffness. The patients suffering from ALS have difficulty in maintaining regular normal locomotion [10]. The earliest signs of ALS include muscles weakness of arms and legs that eventually, prevent the patients from walking and talking and be bedridden. The spreading rate of ALS disease is 1 to 2 per 100,000 each year, most cases of which are sporadic while 5%–10% are inherited. The treatment of ALS is very limited. It becomes necessary to understand the pathological mechanism of this disease.

1.4   The Fall Risk

An important risk factor for NDDs at old age is the increasing fall chances. PD-old patients suffer falls more frequently compared to healthy old people which increase the chances of injuries and may lead to death [9, 11, 12]. Currently, the most common practice to analyze and evaluate the progress of the treatment in NDD patients is mainly based on interviewing the patients. However, depending only on the information

provided by patients can produce misleading data. A more practical and successful approach is to assess the physical functional performance of patients', which helps the physicians to create a more effective treatment plan and more technical assessment of the results of the treatment [1]. Therefore, it is desirable to have a non-invasive wearable continuous gait monitoring system that provides quantitative analysis to detect and classify any movement disorders through monitoring the gait dynamics of the NDD patient. For such system, it is more applicable to utilize wearable sensors with a detection algorithm since it can be used anywhere and not limited to certain location and it does not cause discomfort for the patient.

1.5   Goal of This Work

The primary goal of this work is to study and distinguish the gait dynamics of the NDD patients and compare it with healthy individuals. Specifically, we compare how the three different types of NDDs (PD, HD, and ALS) degrade the patient's ability to control the movement of two feet. This contribution proposes a wearable gait dynamics detection system that will be utilized with foot sensors implanted on the shoe of the patient to analyze the gait dynamics and identify the corresponding NDD disease.

The contribution is structured as follows. First, we give an overview of related work that covers approaches for classifying the gait dynamics in each NDD in Sect. 2. Following this, we explain the proposed Wearable NDD Detection System in Sect. 3. In Sect. 4, we describe the NDD classification algorithm and define a number of comparison criteria in order to show the strengths of our approach. Finally, the results of the discussion are presented in Sect. 5 in which we point out the achieved benefits.

2   Previous Work

The analysis of the gait dynamics of NDD patients has been widely applied for studying movement patterns in NDD patients. Multiple recent studies record the gait dynamics in different NDD patients and extract various features to distinguish each NDD [12–20]. Reference [1] utilized a deterministic learning method that divides the classification process into two phases: a training phase followed by a classification phase using neural networks to categorize the gait dynamics. The gait data of the patients suffering from NDDs were recorded using foot switches with Support Vector Machine (SVM) classifier. The classification results that ALS can be more easily distinguished from PD with an accuracy of 85.47%, HD with an accuracy of 86.52% and the healthy subjects with an accuracy of 93.96% [15]. The swing time series from a patient with PD and a control subject under usual walking conditions were studied in [12] and classified based on Coefficient of variability (CV). Detrended Fluctuation Analysis (DFA) was also used to analyze the fluctuation of the gait cycle based on 200 m walk of 17 PD patients and 12 healthy young people tests as reported in [16]. The least-squares support vector machine (LS-SVM) was used to distinguish the stride patterns between the ALS patients and healthy controls with an accuracy of 82.8% using data recordings from Physionet.org [17]. An Associated Discrete Index (ADI) was defined in [18] in order to measure the discrete degree at the same

frequency. 93 patients with PD and 72 healthy controls were selected. Foot pressure was analyzed including vertical ground reaction force. Power spectra were obtained to compare gait signals of PD and control subjects. Compared with PD patient, the frequency features of gait in control subject are more random, since the spectral lines are loose as well as different with others. On the other hand, those lines in PD patient are comparatively close to each other. This feature can be indicated by ADI, which shows that PD patients always possess larger ADI than that of control subjects [18]. Reference [19] presented an algorithm to analyze a gait pattern in PD patients using deep brain stimulation (DBS). Features were extracted to classify the PD subjects from healthy control subjects with deep brain stimulation (DBS). A mobile sensor based gait analysis system to measure gait patterns in PD and to distinguish mild and severe impairment of gait was proposed in [20–24]. Gait test was performed using sports shoes equipped with inertial sensors. The signals were recorded for both left and right foot, and the features were extracted and classified using different classification algorithm. The sensitivity and specificity were obtained 88% and 86% respectively.

3 Proposed Wearable NDD Detection System

The proposed wearable NDD detection system is composed of a sensing part simulated using CMOS 180 nm technology and a detection algorithm implemented on Field Programmable Gate Array (FPGA) as shown in Fig. 1 [25]. The sensing part is based on Flexi-force resistor (FSR) that measure the force between two surfaces. FSR is robust against most environmental variations [26]. The FSR single element force sensor acts as a force sensing resistor in an electrical circuit. The resistance can be read by connecting a multimeter to the outer two pins, then applying a force to the sensing area. The FSR force sensor is an ultra-thin, flexible printed circuit where the force sensor is constructed of two layers of substrate (polyester/polyamide) film, which does not hinder the normal routine of the person or cause any discomfort. On each layer, a conductive material (silver) is applied, followed by a layer of pressure-sensitive ink. The active sensing area is defined by the silver circle on top of the pressure-sensitive ink. It is renowned for its versatility, ease of integration, and cost-effectiveness. It can be attached to many surfaces and can be combined with plastic or metal films for increased stiffness or for added protection from abrasion. The sensing area is 9.53 mm (0.375 in.) diameter located at the end of the sensor and placed in the shoe sole. It can measure a force ranging up to (1000 lb.) using the readout circuit shown in Fig. 2. In order to measure forces above 100 lb (up to 1000 lb), a lower drive voltage (−0.5 V, −0.25 V, etc.) should be applied with a feedback resistor (1 kΩ min). The FSR data is acquired and processed using Analog Front End (AFE) and then forwarded to NDD classifier to classify the subject's condition as ALS, HD, PD patient or healthy person. The NDD classifier is implemented on FPGA. The processed information will be then transferred to the doctor's/care-giver mobile through Bluetooth/Cloud network associated with the proposed system.
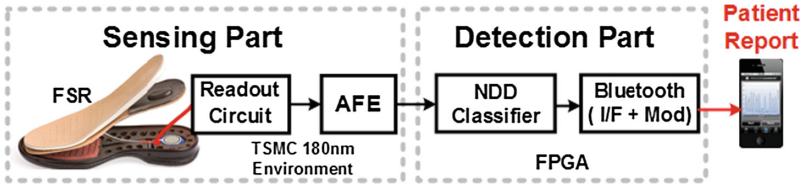
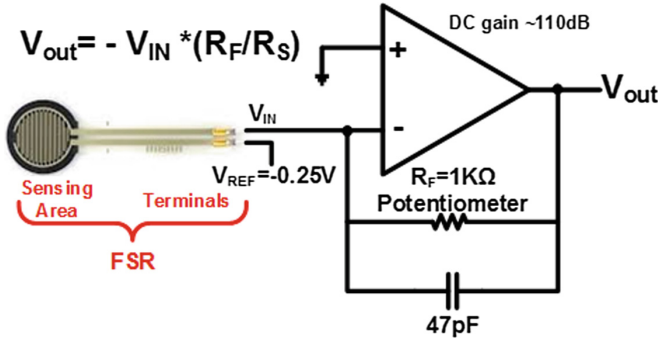**Fig. 1.** System level diagram of the proposed wearable system for the NDD detection.

Fig. 2. FSR Readout circuit to measure more than 100 lb. force.

Figure 3 shows the power comparison of FSR based NDD detection system for two different approaches. Transmitting the FSR raw data for off-sensor processing via a low power Bluetooth interface consumes 1.09 mW [27]. However, if the NDD detection is performed on-sensor, the power consumption is reduced by 72% (0.31 mW), which proofs the advantage of on-sensor processing for the wearable systems [27–29].

The block diagram of the proposed on-sensor wearable NDD classifier and AFE is shown in Fig. 4. The proposed processing system is comprised of Instrumentation Amplifier (AMP) to ensure operating of FSR in the desired weight range, followed by a buffer (BUF), an Analog-to-Digital Converter (ADC), a classifier (detection of disorder), and Bluetooth module/interface for communication with the external world. Since the target is a wearable environment, a 12 bits Successive Approximation (SAR) ADC is utilized as an optimum choice with a sampling rate of 300 Samples/s. The digitized data is then collected and filtered with a median filter to eliminate the noise; followed by an NDD classifier. Based on the captured gait features, the NDD classifier categorize the person into (1) ALS, (2) PD, (3) HD or (4) Normal Person (NP). In addition, the proposed classifier also identifies the severity of the disease.
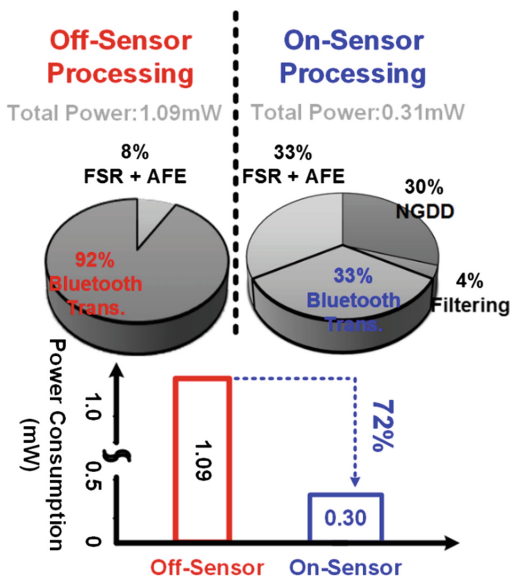
Fig. 3. Power breakdown for two possible on-sensor processing scenarios.
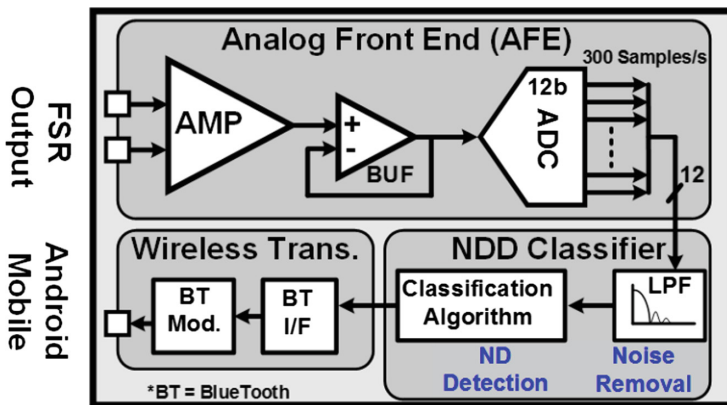

Fig. 4. Block diagram of NDD AFE and the detection processor.

A successive approximation register (SAR) ADC architecture is the natural choice for the wearable/portable biomedical systems [30]. SAR ADC is suited for low speed, moderate resolution, and ultra-low power applications. The designed ADC has a fixed resolution of 12 bits and has a sampling rate of 2.4 kHz. To enhance the common-mode rejection ratio (CMRR) and to eliminate the second order harmonics, a full differential architecture is adopted with the minimal overhead of doubling the digital to analog converter (DAC) power [31]. Figure 5 depicts the architecture of the fully differential ADC which includes differential capacitive DAC, digital comparator, SAR Logic, and switches. The 12b SAR ADC is implemented and simulated using CMOS 180 nm process.
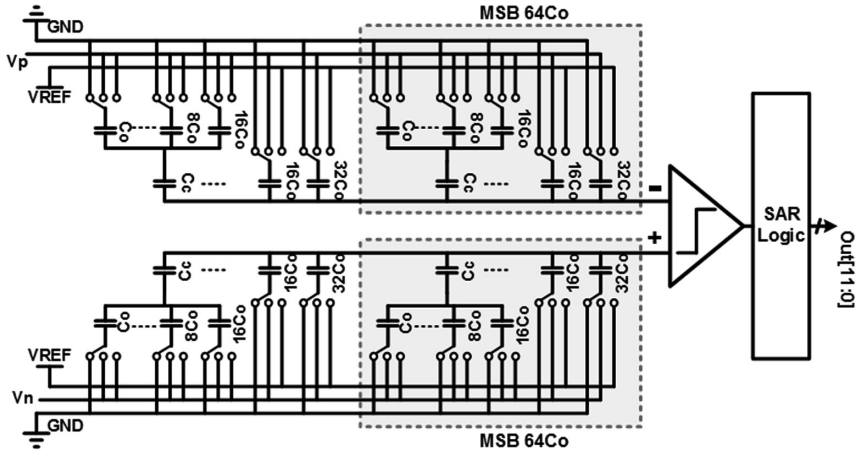
Fig. 5. The architecture diagram of the designed 12b SAR ADC.

The designed 12b SAR ADC utilizes a binary weighted fully differential capacitive DAC. To minimize the power and area consumption sub-DAC and split-capacitor for the most significant bit (MSB) is utilized [32].

The DAC is composed of 7-bit main DAC and 5 bit sub-DAC. The proposed 7/5 division minimize the power consumption while utilizing the same area as 6/6 division. Moreover, 6/6 division suffers from the high differential non-linearity (DNL)/ integral non-linearity (INL) due to the parasitic capacitance on the top plate of the sub-DAC. The MSB capacitor is split into the capacitor array identical to the least significant bit (LSB) capacitor as shown in the Fig. 6.
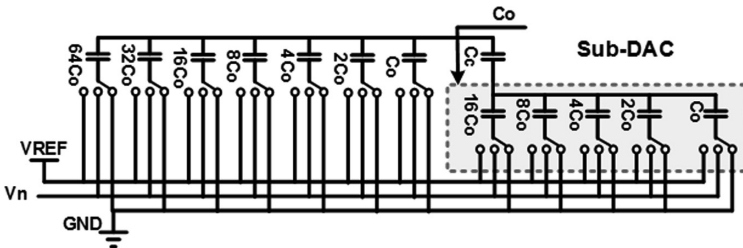

Fig. 6. Binary weighted DAC with 7-bit main-DAC and 5-bit sub-DAC.

The SAR ADC area is mainly dominated by the area of the capacitive DAC. In a binary weighted DAC of N bit resolution, the ratio of MSB to LSB is equal to 2^{N-1}, which is equal to 2048 for 12 bit SAR ADC. To reduce the area of the capacitor array, the capacitive DAC is divided into an M-bit main-DAC and an L-bit sub-DAC that is connected to the main-DAC through a coupling capacitor [33], where the SAR ADC resolution N is equal to M+L. Figure 6 shows the single-sided capacitive DAC split in

M bit main-DAC and L bit sub-DAC where M and L are equal to 7 and 5, respectively, in the implemented design. The coupling capacitor has a value of $2^L Co/2^{L-1}$ which is the 32Co/31. Therefore, the overall effective capacitance of the sub-DAC and coupling capacitor is equal to Co. Figure 7 shows the utilization of superposition principle to depict the effect of voltage V_{TOP} based on each capacitor in the main-DAC and sub-DAC. The effective capacitive divider individually connects the bottom plate of each capacitor in the main-DAC V_{REF}. First, if the bottom plate of the MSB capacitor (64 Co) is connected to V_{REF} and the bottom plate plates of the rest of the capacitors are connected to the GND. A capacitive divider with two capacitors each is equal to 64-Co occurs and voltage V_{TOP} is equal to half the V_{REF} value. If the capacitor 32Co is the one connected to V_{REF} instead the voltage is equal to quarter V_{REF} and so on.
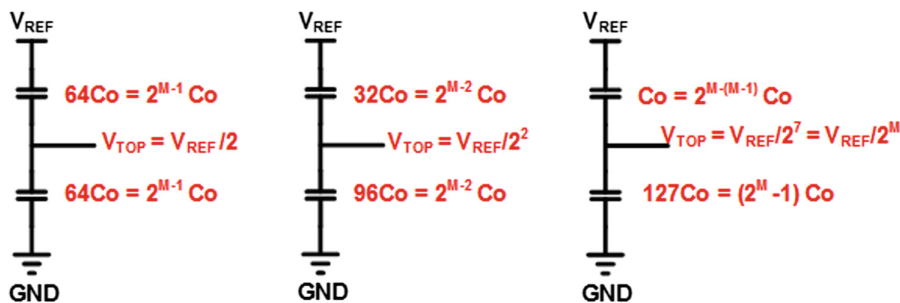

Fig. 7. Explanation of the DAC effective capacitive divider while individually connecting the bottom plate of each capacitor in the main-DAC to V_{REF} and the rest of capacitors to GND.

Thevenin equivalent is utilized to apply same procedure for the sub-DAC evaluation. Figure 8 shows the effective capacitive divider while connecting the bottom plate of the MSB capacitor of the sub-DAC to V_{REF} and the rest of capacitors to the GND. The voltage V_{TOP} is equal to $V_{REF}/2$ divided by 2M which is the half the value yielded by the LSB of main-DAC. The same analysis can be applied to the rest of the capacitors of the sub-DAC. It should be noted the Thevenin equivalent capacitance shown in Fig. 8 is the same while switching any of sub-DAC capacitors.
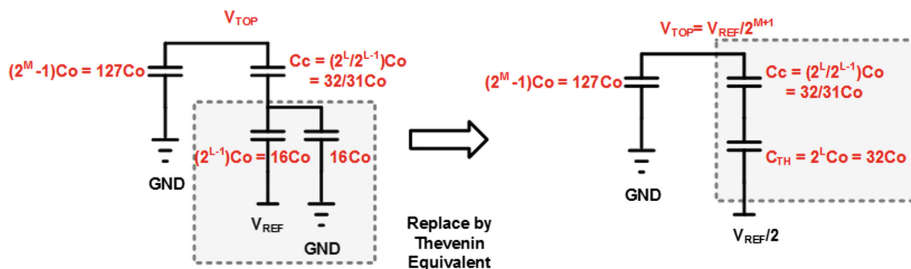

Fig. 8. Thevenin equivalent circuit for analyzing passive sub-DAC.

The only problem with sub-DAC interpolation is its sensitivity to the parasitic capacitance at the top plate of sub-DAC capacitors. This leads to INL/DNL errors due to the compression of transition steps by the sub-DAC. However, this problem can be compensated by an increase in the size of the coupling capacitor by RTP [33] as given in the following equation where C_P is the extracted parasitic capacitance from the top plate of subDAC to GND and $C_{sub\ DAC}$ is the total capacitance of the sub-DAC which is equal to $2^L Co$ (32 Co in this case).

$$R_{RP} = 1 + \frac{C_P}{C_{subDAC}} \tag{1}$$

To reduce the power consumption, dynamic comparators are utilized which are highly power efficient and thus cut down one of the main sources of power dissipation in the SAR ADC. The two main problems of this type of comparators are the input-referred offset and kick-back noise. The transistors are sized to keep the 3σ offset close to 50 mV. Kickback noise has little effect on the operation of the ADC as it roughly common mode when the outputs begin to rise [33]. The SAR Logic is responsible for generating the switch control signals during the different phases of operations. The SAR logic consists of three main blocks, first the sequencer for providing timing control. It sets the period of purging, sampling and bit-cycling and timing for latching the output of the comparator. The second part is the data register which is used to store the output of digital comparator during the bit-cycling phase to form the digital output vector. The third part utilizes outputs of the sequencer and data register to generate the switches control signals of the main-DAC and sub-DAC.

The performance summary of implemented SAR ADC is shown in Table 1. The SAR ADC achieves an effective number of bits (ENOB) of 11.4, signal-to-noise-distortion ratio (SNDR) of 60 dB, spurious free dynamic range (SFDR) of 72 dBFS which provides information about the difference between maximum amplitude tone in frequency spectrum and the fundamental input tone, DNL and INL of 0.275 LSB and 0.3 LSB, respectively, which gives deviation of actual conversion from the ideal one.

Table 1. 12b SAR ADC performance summary.

Power consumption	57 nW
ENOB	11.4
SNDR	60 dB
SFDR	72 dB
DNL	0.275 LSB
INL	0.3 LSB

4 NDD Classification Algorithm

The main goal is to extract the discriminating features to classify the different NDDs. The gait cycle duration (known as stride-time), is considered as one of the main features to identify person's gait dynamics [1]. The heel strike is defined as the heel

first touches the ground and ends until the whole foot touches the ground. As shown in the Fig. 9, the early flatfoot strike occurs, when the whole foot is on the ground. The late flatfoot stages end when the heel lifts off the ground. The rise begins when the heel starts to leave the ground. The toe-off phase occurs when the toe leaves the ground. 60% of the walking consists of stance phase. The Stance phase occurs when the whole foot is on the ground. Swing phase is basically defined as the one foot is on the ground and the other is in the air. Figure 10 shows the digitized FSR output from the ADC for an ALS patient for a duration of 100 s along with right and left stride intervals in red and blue, respectively. Close analysis of the graph shows that stride interval of both left and right foot gives same information about the human behavior. Moreover, the left stride time seems to be more sensitive and gives more details in comparison to the right. These results are consistent among all the patients (ALS, HD, PD) and therefore in this work only left stride is utilized in the processing to save power and area utilization.
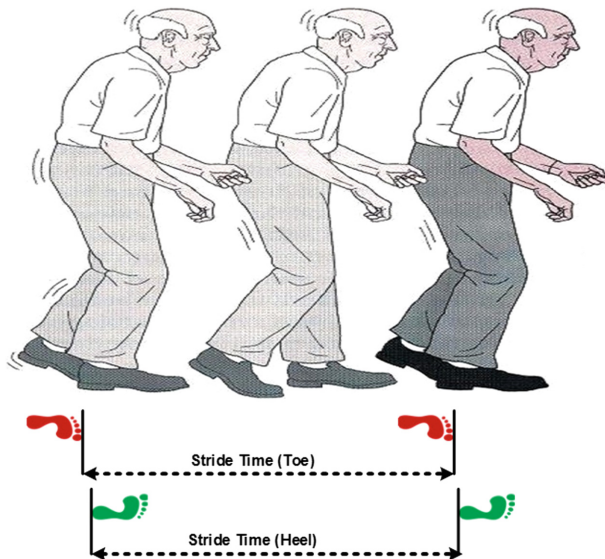

Fig. 9. Gait abnormality in neurodegenerative diseases and stride time.

Figure 11 shows the average left stride time interval for different NDD i.e. ALS, PD, HD and NP. Subjects with ALS, have longer average stride time interval compared with that of the HD, PD and the healthy subjects. Therefore, the average stride time interval is an effective feature for the NDD detection that is used in our proposed NDD classifier. It is also observed that the stride-time interval is a key feature to distinguish between ALS and other NDDs based on Fig. 11. Another important feature for NDD detection is the stride-time fluctuation w.r.t corresponding mean which is more dominant in the HD relative to other NDDs [23] except ALS as shown in the Fig. 12.

But the ALS can be detected based on stride time, therefore stride time fluctuations can be treated as a feature for the HD detection. Stride time fluctuation is calculated by taking the derivative of the stride time and the Fig. 12 shows the relative maximum and continuous fluctuation in the stride time compared to the NP, ALS, and PD.
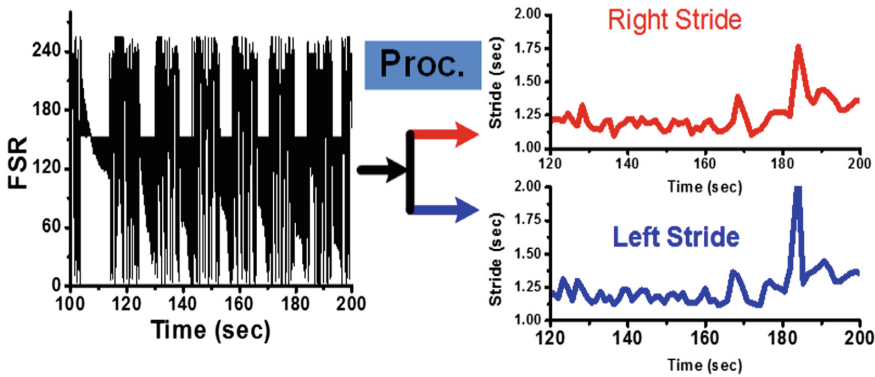

Fig. 10. Digitized FSR output with extraction into left and right stride time. (Color figure online)

The selection of stride time fluctuation as feature reduces the overall feature set compared to [1] and [12] by more than 60%. Furthermore, to discriminate the PD and NP, a detailed analysis is performed to carefully select feature which significantly distinguishes the PD from NP. For this purpose, the autocorrelation of the decay time for the NDD is done with the healthy subject, and the value came out to be greatest for the PD patients. Therefore, the autocorrelation is also considered as a discriminatory feature for the PD patients.
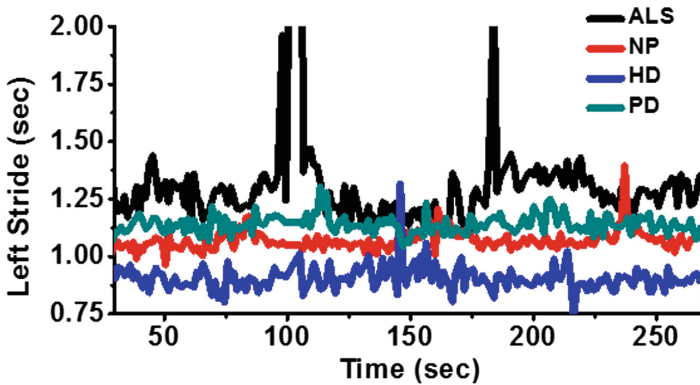

Fig. 11. Average stride time comparison of different NDD (ALS, PD, HD) and NP.

Figure 13 shows the computed auto-correlation factor value of different NDD's used in this work. The values show ALS achieves maximum value but since stride time alone is enough to determine the ALS, therefore, stride time along with auto-correlation factor discriminate PD from all other NDD's and NP with good classification accuracy, since PD has the second maximum value of auto-correlation factor among NP and HD.
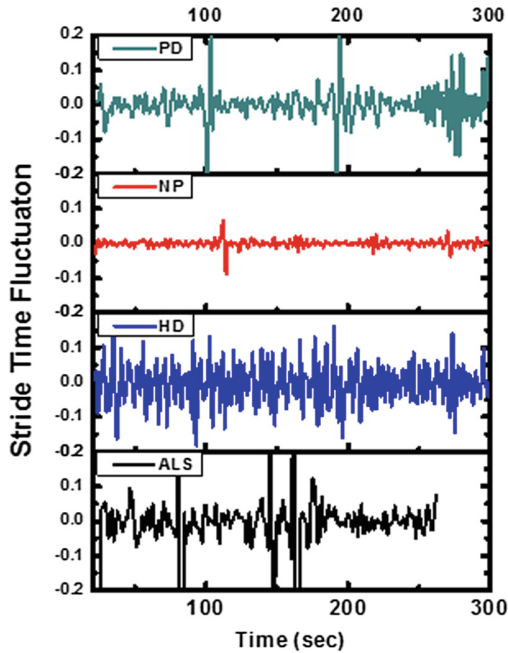

Fig. 12. Average stride time fluctuation comparison of different NDD (ALS, PD, HD) and NP.
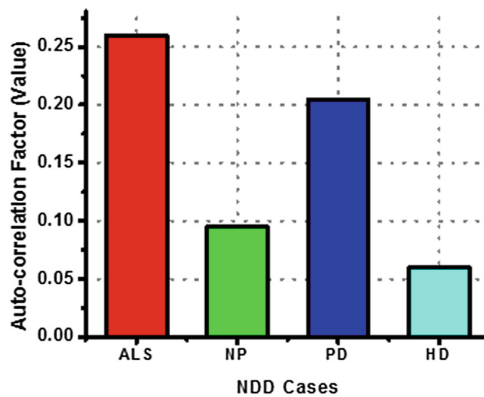

Fig. 13. Average auto-correlation factor comparison of different NDD (ALS, PD, HD) and NP.

Figures 14 and 15 shows the state flow diagram and the algorithm for the proposed NDD classification method based on 3 features: (1) stride-time, (2) fluctuation in the stride time and (3) autocorrelation decay factor. The stride time value is the duration of gait cycle which is the time interval between two consecutive heel strikes of the same foot in milliseconds. Fluctuation in the stride time is an indication of the inconsistent limb movements. Therefore, the mean and standard deviation of stride time are utilized to estimate the fluctuation variation value (FVV). The FVV can be considered as a measure of the variability of temporal stride dynamics caused by the imbalanced rhythmic walking mechanism. Low FVV indicates automated rhythmic characteristics of gait dynamics and is utilized by physicians as a clinical index for stable gait dynamics. FVV among healthy individuals is low and usually below 3% [34]. Explicitly can be determining a factor for ALS and HD patients. The autocorrelation function indicates how the stride time series of each patient is correlated with itself over different time delays and gives a measure of the memory in the system. The auto-correlation decay-time value (ADV) is defined as the number of strides required for the autocorrelation of the stride time series to fall to 63% $(1 - 1/e)$ of its initial value [35].
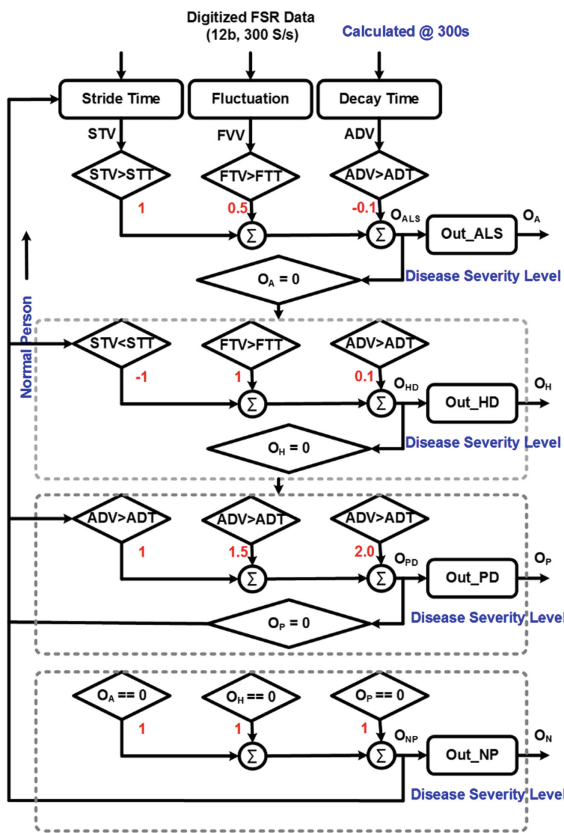

Fig. 14. State flow diagram of the proposed NDD classifier.

The O_A, O_H, O_P, and O_N are outputs of corresponding NDD and their values are calculated based on the STV (Stride time value), FVV, and ADV (Autocorrelation decay-time value) in relation to the STT (Stride time threshold), FVT (Fluctuation variation threshold), and ADT (Autocorrelation decay-time threshold). The detection time for one cycle of evaluation is 5 min (300 s) and will continue repeating if NDD goes undetected.

Algorithm Proposed NDD Classification Algorithm

1: **Input:** STV, STT, FVV, FVT, ADV, and ADT
2: **Output:** O_A, O_H, O_P, O_N
3: **for** the kth iteration **do**
4:     Load the original 300 sec data
5:     $O_{ALS} \leftarrow (STV > STT) + 0.5 * (FVV > FVT) - 0.1 * (ADV > ADT)$
6:     **if** $O_{ALS} \leq 0.5$ **then**
7:         $O_A \leftarrow 0$
8:     **else if** $O_{ALS} > 0.5$ and $O_{ALS} < 1.0$ **then**
9:         $O_A \leftarrow 1$
10:     **else if** $O_{ALS} > 1$ and $O_{ALS} < 1.4$ **then**
11:         $O_A \leftarrow 2$
12:     **else**
13:         $O_A \leftarrow 3$
14:     **end if**
15:     **if** $(O_A = 0$ or $O_A = 3)$ **then**
16:         Load the original 300 sec data
17:         $O_{HD} \leftarrow (FVV > FVT) - 1 * (STV < STT) + 0.1 * (ADV > ADT)$
18:         **if** $(O_{HD} > -0.2$ and $O_{HD} < 0.2)$ **then**
19:             $O_H \leftarrow 0$
20:         **else if** $O_{HD} > 0.9$ **then**
21:             $O_H \leftarrow 2$
22:         **else**
23:             $O_H \leftarrow 3$
24:         **end if**
25:     **end if**
26:     **if** $(O_H = 0$ or $O_H = 3)$ **then**
27:         Load the original 300 sec data
28:         $O_{PD} \leftarrow (ADV > ADT) + (ADV > 1.5 * ADT) + (ADV > 2 * ADT)$
29:         **if** $O_{PD} = 0$ **then**
30:             $O_P \leftarrow 0$
31:         **else if** $O_{PD} = 1.0$ **then**
32:             $O_H \leftarrow 1$
33:         **else if** $(O_{PD} > 1.0$ and $O_{PD} < 2.6)$ **then**
34:             $O_P \leftarrow 2$
35:         **else**
36:             $O_P \leftarrow 3$
37:         **end if**
38:     **end if**
39: **end for**
40: **if** $(O_A = 0$ and $O_H = 0$ and $O_P = 0)$ **then**
41:     $O_N \leftarrow 1$
42: **else**
43:     $O_N \leftarrow 0$
44: **end if**

Fig. 15. Proposed NDD classification algorithm.

Additionally, based on threshold level and the proposed NDD algorithm, the two bits output of the classifier also describe the severity of the corresponding disorder. If none of the diseases is detected, the patient will be claimed as a normal scenario. Since it's also important to detail severity level of ND and action item, therefore the relation of NDD output, the severity of the disorder and corresponding action are detailed in Table 2. This information will be presented to the concerned person himself, caregiver and physician via cloud/Bluetooth link. The NDD classifier output is 2 (two)-bit with binary encoding utilized for each corresponding NDD, for example, the 2'b11 means a high score of specific NDD, meaning the person has the severe symptom of that NDD and needs to take precautionary measures on urgent basis.

Table 2. NDD output with score description and action item.

NDD Output	Score Description	Action Item
2'b00	Low Score of NDD	Need to monitor Situation
2'b01	Medium Score of NDD	Need to visit Doctor
2'b11	High Score of NDD	Emergency Situation
2'b10	Not enough data	Need further analysis

To form a mathematical model for the detection based on the above discrimination, the fall detection algorithm is as follows. The decision weights are carefully selected based on the rigorous simulation for the Neuro-Degenerative Disease Data Base [35].

5   Results and Discussion

The system is verified with the Gait Dynamics in Neuro-Degenerative Disease Data Base 35, which contains 64 subjects having ALS, HD, PD and Healthy Subjects of 13, 20, 15 and 16, respectively. To measure the real-time performance and working, the complete implementation is also done on FPGA. The average overall classification accuracy was computed using the Xilinx Virtex 5 LX-110T FPGA board and Logic analyzers were used to display and verify the NDD classification. The sensitivity and specificity are defined by (2) and (3), respectively, along with the definition of True Positive, True Negative, False Positive, and False Negative in (4)–(7).

$$Sensitivity = \frac{True \; Positive}{True \; Positive + False \; Negative} \tag{2}$$

$$Specificity = \frac{True \; Negative}{False \; Positive + True \; Negative} \tag{3}$$

$$True \; Positive = \frac{\# \; of \; pattern \; classified \; Normal}{Total \; \# \; of \; Normal \; Patterns} \tag{4}$$

$$True \; Negative = \frac{\# \; of \; pattern \; classified \; Abnormal}{Total \; \# \; of \; Abnormal \; Pattern} \tag{5}$$

$$False \; Negative = \frac{\# \; of \; pattern \; classified \; Abnormal}{Total \; \# \; of \; Normal \; Pattern} \tag{6}$$

$$False \; Positive = \frac{\# \; of \; pattern \; classified \; Normal}{Total \; \# \; of \; Abnormal \; Pattern} \tag{7}$$

The evaluation shows the proposed system achieves an averaged sensitivity and specificity of 90.8% and 94.5%, respectively for total 64 subjects. The verification results of the proposed system are shown in Fig. 16. It also achieves a classification accuracy of 93.8%, 89.1%, 94% and 93.3%, for ALS, HD, PD, and normal person, respectively.
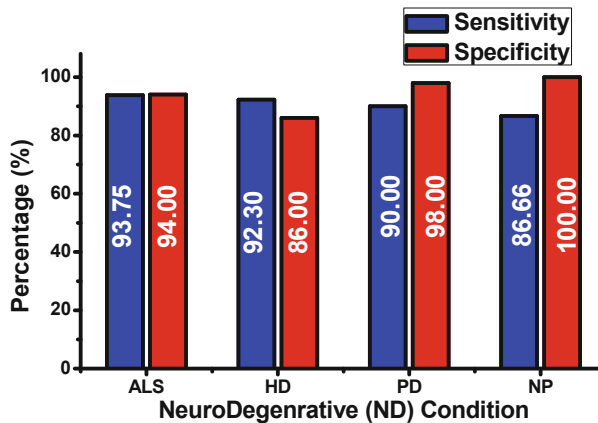

Fig. 16. Measured sensitivity and specificity of NDD.

Figure 17 shows the performance of the proposed system, the digitized FSR data is processed to evaluate the stride time and based on the stride time, fluctuation in the stride and autocorrelation decay time; the specific NDD is determined and the final information is transferred to the doctor/caretaker mobile via Bluetooth. Different

scenarios are shown in the Fig. 17 for the working of the proposed NDD classification system along with the computed values (STV, ADV, and FVV) and their corresponding threshold values (STT, ADT, and FVT). The message showing the severity level of the disease along with proposed action item is displayed on caregiver or physician smartphone through a low-energy Bluetooth link. Table 3 compares the performance of the proposed NDD processor with the state-of-the-art works. All other works focus on software implementation only whereas this work target a wearable device with on-sensor processing. It also utilizes only 3 features to distinguish between the different NDDs and healthy persons. The system achieves an overall sensitivity, specificity and classification accuracy of 90.8%, 94.5%, and 92.9%, respectively. Since the proposed system is targeting a wearable environment, therefore an area and power efficient 12b-SAR ADC are implemented using 65 nm CMOS technology consuming <60 nW.
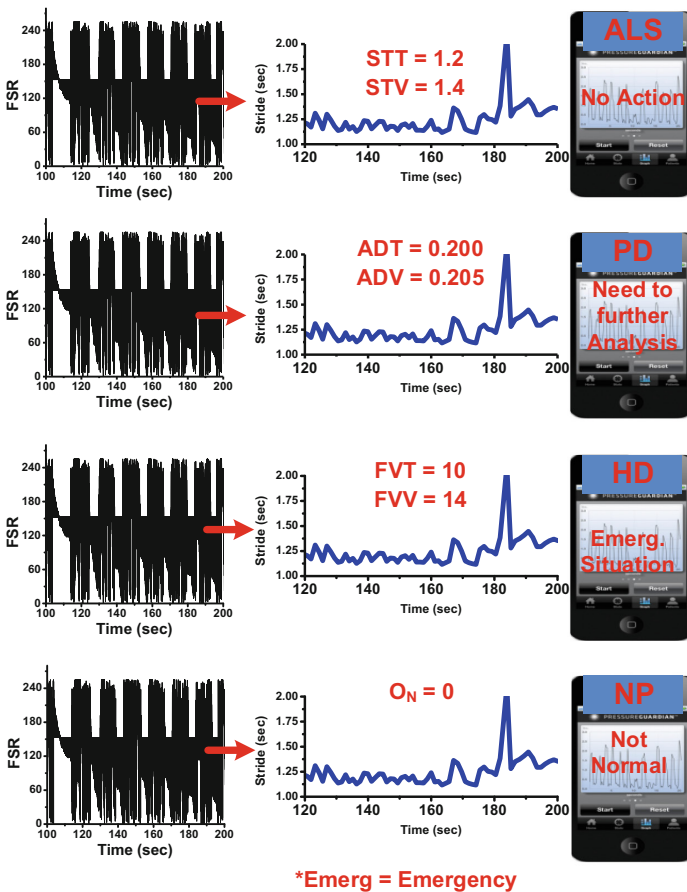

Fig. 17. The measured result showing the system working.

Table 3. Comparison with state-of-the-art works.

Parameter	Zeng [1]	Ren [2]	Wu [17]	Barth [20]	Aziz [21]	This work
Sensor type	FSR	FSR	FSR	Inertial sensors	FSR	FSR
Sensor location	Foot	Foot	Foot	Foot	Foot	Foot
On sensor detection	X	X	X	X	X	O
No. of features	12	10	1	12	1	3
Avg. sensitivity	91.7%	93.7%	76.9%	88%	89.3%	90.8%
Avg. specificity	100%	78.3%	87.5% [20–24]	86%	78.3%	94.5%
Target application	NDD	NDD	ALS	PD	NDD	Wearable: NDD

6   Conclusion

This contribution proposes a wearable novel NDD detection system for the detection and classification of ALS, HD, and PD. The proposed system is based on the minimum feature set of 3 features which will ensure lower power and area implementation without affecting the overall detection performance. The proposed system aims to provide a solution for the next generation of miniaturized wearable devices to detect the NDD at an early stage and may help in reducing the severity of NDD. The proposed system is tested on patient's recordings from Physionet Gait Dynamics dataset and achieves a classification accuracy of 93.8%, 89.1%, 94% and 93.3%, for ALS, HD, PD, and healthy person, respectively, from a total set of 64 subjects.

References

1. Zeng, W., Wang, C.: Classification of neurodegenerative diseases using gait dynamics via deterministic learning. J. Inf. Sci. **317**(1), 246–258 (2015)
2. Ren, P., Zhao, W., Zhao, Z., Bringas-Vega, M.L., Valdes-Sosa, P.A., Kendrick, K.M.: Analysis of gait rhythm fluctuations for neurodegenerative diseases by phase synchronization and conditional entropy view document. IEEE Trans. Neural Syst. Rehabil. Eng. **24**(2), 291–299 (2016)
3. Scafetta, N., Marchi, D., West, B.J.: Understanding the complexity of human gait dynamics. Chaos **19**(2), 026108–026110 (2009)
4. Banaie, M., Pooyan, M., Mikaili, M.: Introduction and application of an automatic gait recognition method to diagnose movement disorders that arose of similar causes. Expert Syst. Appl. **38**(6), 7359–7363 (2011)

5. Parkinson's disease Foundation: Statistics. http://parkinson.org/Understanding-Parkinsons/Causes-and-Statistics/Statistics
6. Huntington Disease: Health Conditions, June 2013. https://ghr.nlm.nih.gov/condition/huntington-disease#statistics
7. National Institute of Neurological Disorders and Stroke: Huntington's disease information page. https://www.ninds.nih.gov/Disorders/All-Disorders/huntingtons-Disease-Information-Page
8. Hausdorff, J.M., et al.: Altered fractal dynamics of gait: reduced stride-interval correlations with aging and Huntington's disease. J. Appl. Physiol. **82**(1), 262–269 (1997)
9. Grimbergen, Y.A., Knol, M.J., Bloem, B.R., Kremer, B.P., Roos, R.A., Munneke, M.: Falls and gait disturbances in Huntington's disease. Mov. Disord. **23**(7), 970–976 (2008)
10. US San Diego, School of Medicine: Center for ALS Research and Therapy. http://als.ucsd.edu/about-als/Pages/incidence.aspx
11. Saadeh, W., Altaf, M.A.B., Altaf, M.S.B.: A high accuracy and low latency patient-specific wearable fall detection system. In: Proceedings of the IEEE International Conference on Biomedical Health Informatics, BHI, pp. 441–444, February 2017
12. Balash, Y., Peretz, C., Leibovich, G., Herman, T., Hausdorff, J.M., Giladi, N.: Falls in outpatients with Parkinson's disease: frequency, impact, and identifying factors. J. Neurol. **252**(11), 1310–1315 (2005)
13. Hausdorff, J.M.: Gait dynamics, fractals and falls: finding meaning in the stride-to-stride fluctuations of human walking. J. Hum. Mov. Sci. **26**(4), 555–589 (2007)
14. Saadeh, W., Habte, T., Perrott, M.: A > 89% efficient LED driver with 0.5 V supply voltage for applications requiring low average current. In: Proceedings of the IEEE Asian Solid-State Circuits Conference, A-SSCC, pp. 273–276, November 2013
15. Yang, M., Zheng, H., Wang, H., McClean, S.: Feature selection and construction for the discrimination of neurodegenerative diseases based on gait analysis. In: Proceedings of the International Conference on Pervasive Computing Technologies for Healthcare, pp. 1–7 (2009)
16. Ota, L., Uchitomi, H., Suzuki, K., Hove, M.J., Orimo, S., Miyake, Y.: Relationship between fractal property of gait cycle and severity of Parkinson's disease. In: Proceedings of the IEEE/SICE International Symposium on System Integration, SII, pp. 236–239, December 2011
17. Wu, Y., Ng, S.C.: A PDF-based classification of gait cadence patterns in patients with amyotrophic lateral sclerosis. In: Proceedings of the IEEE Engineering in Medicine and Biology Conference, EMBC, pp. 1304–1307, August 2010
18. Han, Y., Ma, Z., Zhou, P.: A study of gaits in Parkinson's patients using Autoregressive model. In: IEEE Proceedings, pp. 104–107 (2009)
19. Fatmehsari, Y.R., Bahrami, F.: Assessment of Parkinson's disease: classification and complexity analysis. In: Proceedings of the Iranian Conference of Biomedical Engineering, pp. 1–4 (2010)
20. Barth, J., et al.: Biometric and mobile gait analysis for early diagnosis and therapy monitoring in Parkinson's disease. In: Proceedings of IEEE Engineering in Medicine and Biology Society, EMBS, pp. 868–871, September 2011
21. Aziz, W., Arif, M.: Complexity analysis of stride interval time series by threshold dependent symbolic entropy. Eur. J. Appl. Physiol. **98**(1), 30–40 (2006)
22. Daliri, M.R.: Chi-square distance kernel of the gaits for the diagnosis of Parkinson's disease. Biomed. Signal Process. Control **8**(1), 66–70 (2013)
23. Dillmann, U., et al.: Principal component analysis of gait in Parkinson's disease: relevance of gait velocity. Gait Posture **39**(3), 882–887 (2014)

24. Huang, A., Mallet, L.: Medication-Related Falls in Older People: Causative Factors and Management. Springer, Heidelberg (2016). https://doi.org/10.1007/978-3-319-32304-6
25. Saadeh, W., Altaf, M.A.B., Butt, S.: A wearable neuro-degenerative diseases classifier system based on gait dynamics. In: IFIP/IEEE International Conference on Very Large Scale Integration, VLSI-SoC, pp. 1–6, October 2017
26. Flex Sensor. https://www.tekscan.com/products-solutions/force-sensors/a201
27. Saadeh, W., Alsuradi, H., Altaf, M., Yoo, J.: A 1.1 mW ground effect-resilient body coupled communication transceiver with pseudo OFDM for head and body area network. IEEE J. Solid-State Circuits (JSSC) **52**(10), 2690–2702 (2017)
28. Saadeh, W., Kifle, Y., Yoo, J.: A hybrid OFDM body coupled communication transceiver for binaural hearing aids in 65 nm CMOS. In: Proceedings of the IEEE International Symposium on Circuits and Systems, ISCAS, pp. 2620–2623, May 2015
29. Saadeh, W., Alsuradi, H., Altaf, M.A.B., Yoo, J.: A 1.1 mW hybrid OFDM ground effect-resilient body coupled communication transceiver for head and body area network. In: Proceedings of the IEEE Asian Solid-State Circuits Conference, ASSCC, pp. 201–204, November 2016
30. Altaf, M.A.B., Zhang, C., Yoo, J.: A 16-channel patient-specific seizure onset and termination detection SoC with impedance-adaptive transcranial electrical stimulator. IEEE J. Solid-State Circuits (JSSC) **50**(11), 2728–2740 (2015)
31. El-Damak, D.R.: Design of ultra low power analog-to-digital converter for ambulatory EEG recording. M.S. thesis, Massachusetts Institute of Technology, Cambridge (2012)
32. Yazicioglu, R.F., Merken, P., Puers, R., Hoof, C.V.: A 200 pw eight-channel acquisition ASIC for ambulatory EEG systems. In: IEEE International Solid-State Circuits Conference on Digest of Technical Papers, pp. 164–165, February 2008
33. Verma, N.: An ultra-low power ADC for wireless micro-sensor applications. M.S. thesis, Massachusetts Institute of Technology, Cambridge, MA, June 2005
34. Beauchet, O., et al.: Walking speed-related changes in stride time variability: effects of decreased speed. J. NeuroEng. Rehabil. **6**, 32 (2009)
35. Hausdorff, J.M., et al.: Dynamic markers of altered gait rhythm in amyotrophic lateral sclerosis. J. Appl. Physiol. **88**(6), 2045–2053 (2000)